THE JOURNAL OF PHYSICAL CHEMISTRY A

Article

Cite This: J. Phys. Chem. A 2018, 122, 2983−2991

pubs.acs.org/JPCA

Titanium Insertion into CO Bonds in Anionic Ti−CO_2 Complexes

Leah G. Dodson,[†] Michael C. Thompson,[‡] and J. Mathias Weber*[,‡]

[†]JILA and NIST and [‡]JILA and Department of Chemistry and Biochemistry, University of Colorado, 0440 UCB, Boulder, Colorado 80309-0440, United States

Supporting Information

ABSTRACT: We explore the structures of $[Ti(CO_2)_y]^-$ cluster anions using infrared photodissociation spectroscopy and quantum chemistry calculations. The existence of spectral signatures of metal carbonyl CO stretching modes shows that insertion of titanium atoms into C−O bonds represents an important reaction during the formation of these clusters. In addition to carbonyl groups, the infrared spectra show that the titanium center is coordinated to oxalato, carbonato, and oxo ligands, which form along with the metal carbonyls. The presence of a metal oxalato ligand promotes C−O bond insertion in these systems. These results highlight the affinity of titanium for C−O bond insertion processes.

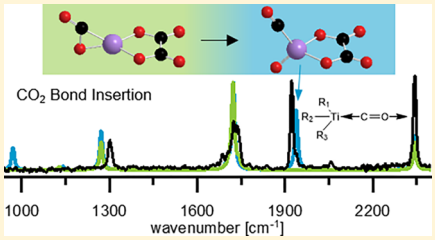

INTRODUCTION

Adsorption of CO_2 on neutral TiO_2 surfaces has been shown to result in C−O bond dissociation and the formation of gaseous or surface-adsorbed CO upon the addition of an excess electron.[1,2] This reaction is thought to proceed at titanium atoms next to oxygen vacancy sites, where the newly formed O^- atomic ion can fill the vacancy. This hypothesis involving an undercoordinated titanium atom as an active site is reminiscent of supported single-atom catalyst systems, where single metal atoms are anchored to high surface area supports (e.g., zeolites, metal organic frameworks) or incorporated in surface-immobilized metal−organic complexes.[3−5] In these systems, access by reactant molecules to the catalyst is controlled by the (incomplete) coordination environment of the metal center.

Elucidating the structural motif for the interaction of CO_2 with a metal center of a heterogeneous catalyst in situ is challenging due to surface inhomogeneity and speciation, particularly under turnover conditions, where multiple species will be present. Infrared spectroscopy has been used with some success to suggest binding motifs for CO_2 molecules interacting with a TiO_2 surface, but these studies do not take into consideration the effect that an excess electron would have on the metal−CO_2 moiety.[6−10] An alternative route to the detailed characterization of metal−molecule interaction is to use mass spectrometric preparation of ionic complexes in tandem with laser spectroscopy. Such a strategy circumvents many of the complications of speciation and allows the detailed study of model systems for metal−CO_2 interaction.[11−17]

As an example of more extreme undercoordination, the interaction of CO_2 with bare, atomic Ti and molecular TiO_x (x = 1−2) has been studied in experimental and computational work on gas-phase and matrix-isolated titanium and titanium oxide neutrals and cations, investigating the structure of CO_2-single metal atom complexes and the activation that occurs.[18−25] Notably, this work showed that insertion of Ti into C−O bonds occurs for neutral Ti and TiO reactions with CO_2,[18,21−26] as well as for Ti^+ with CO_2.[27,28] In fact, Mascetti and co-workers demonstrated that a Ti atom spontaneously inserts into CO_2 with no barrier, forming a strong TiO bond and a metal carbonyl.[22,24] Early transition metals, with their high oxophilicities, are generally likely to form insertion products in interaction with CO_2, due to the strength of the formed metal−oxygen bond.[28] Other works have shown CO bond insertions in cationic clusters of CO_2 with titanium and vanadium, as well as silicon and nickel.[29−33]

The behavior of negatively charged complexes of Ti and CO_2 involving these processes has not been studied, yet it is highly relevant in the context of electroreduction of CO_2. Similarly, the influence of coordination and ligands on the propensity for bond insertion has not been clearly addressed. In the present work, we investigate the structure of clusters of a single titanium atom interacting with CO_2 molecules in the presence of an excess electron using photodissociation spectroscopy of mass-selected, metal-containing cluster ions[34] in concert with quantum chemical calculations. We allow multiple CO_2 molecules to interact with the metal, observing evidence for bond insertion products as well as formation of other CO_2-based ligands. Finally, we computationally explore the impact of a ligand on C−O bond insertion in $[Ti(CO_2)_y]^-$ clusters and discuss the influence of charge on the intracluster chemistry in Ti−CO_2 clusters.

EXPERIMENTAL AND COMPUTATIONAL METHODS

Experiments are carried out with an infrared photodissociation spectrometer described previously.[34] Briefly, material from a rotating titanium metal disc target is vaporized by the third harmonic of an Nd:YAG laser (355 nm, 35−40 mJ $pulse^{-1}$). The metal vaporization plasma is entrained in a supersonic expansion of CO_2 (5.5 bar backing pressure) emitted by a

Received: February 22, 2018
Revised: March 5, 2018
Published: March 7, 2018

DOI: 10.1021/acs.jpca.8b01843
J. Phys. Chem. A 2018, 122, 2983−2991

pulsed Even–Lavie valve. The resulting metal–CO_2 clusters are injected into a Wiley–McLaren time-of-flight mass spectrometer, and ion optics steer the cluster anions through differentially pumped regions to the first space focus of the mass spectrometer, where ions with the mass-to-charge ratio (m/z) of interest are isolated by a pulsed mass gate.[35] The mass-selected ions are irradiated with the output of a pulsed, tunable infrared light source, with signal enhancement achieved using a multipass optical configuration.[36] Photodissociation occurs when the infrared laser is resonant with a vibrational transition in the anionic cluster and imparts sufficient energy to evaporate a subcomponent of the cluster. This method of detecting absorption events relies on the presence of weakly bound CO_2 molecules, whose binding energies are on the order of or less than the energy of the absorbed photon.

The experimental spectrum is collected in two parts (940–2160 and 2085–2400 cm^{-1}), corresponding to two different crystal settings of the infrared optical parametric converter, with nearly 100 cm^{-1} of overlap between the two spectral regions. In the spectra collected for this work, this overlap region contains an absorption band whose peak area, as fitted with a Lorentzian, is used to scale the two regions relative to each other.

In order to interpret the experimental data, we use density functional theory calculations to find minimum energy structures of $[Ti(CO_2)_y]^-$ cluster anions (y = 4 and 5) and predict their infrared spectra. All geometry optimization calculations are performed with the TURBOMOLE quantum chemical program[37] using the B3LYP density functional[38,39] with empirical dispersion correction[40] and the def2-TZVPP basis set.[41] This level of theory has been successfully used in past work on metal–CO_2 anionic clusters.[42−50]

An empirical scaling factor of 0.9754 was used to qualitatively account for anharmonicity and to scale computed CO_2 vibrations, based on previous work in our group on the stretching oscillations of CO_2-based ligands.[42−50] In order to derive a scaling factor that is valid for carbonyl stretching vibrations, we compared the vibrational frequencies obtained using our methods with experimental work on $[Ti(CO)_6]^+$ by Brathwaite et al.[14] This work investigated the metal-dependent shift of the carbonyl stretching vibration, identifying a single band in the $[Ti(CO)_6]^+$ experimental spectrum at $\nu_{CO,expt}$ = 2110 cm^{-1}, which they assign to a quartet O_h cluster. Using the same methods described above (B3LYP-disp/def2-TZVPP level and basis), we reoptimized the quartet O_h $[Ti(CO)_6]^+$ geometry and obtained the vibrational frequencies (see Tables S5 and S6) for this cation. The unscaled calculated value for $\nu_{CO,theor}$ is 2177 cm^{-1}, resulting in a scaling factor ($\nu_{CO,expt}/\nu_{CO,theor}$) = 0.9692. All calculated CO stretching modes of carbonyl groups were multiplied by this factor for the purpose of comparing the experimentally observed infrared spectrum with the calculated structures. The computed infrared spectra are convolved with a 12 cm^{-1} fwhm Lorentzian line shape to produce predicted spectra for comparison with our experimental results.

A Natural Bond Orbital analysis is carried out using NBO 5.0,[51] as implemented in Q-Chem, Version 4.0.1.[52] These calculations operate at the B3LYP level with the same empirical dispersion correction referenced above, the def2-TZVPP basis for C and O atoms, and the def-TZVPP basis for metal atoms. Natural populations and Mulliken–Mayer bond orders are extracted from these calculations.

RESULTS AND DISCUSSION

Spectroscopy of $[Ti(CO_2)_n]^-$ Cluster Ions. In metal–CO_2 cluster anions, CO_2 units can exist in one of two roles. They can be covalently bound to the metal and be characterized as a part of the core ion of the cluster or they can be weakly bound to the core ion and play the role of a solvent (note that individual "CO_2 units" may no longer have the connectivity of CO_2, hence the use of the word "units"). The experimental strategy employed here relies on the presence of a weakly bound species, since absorption of a single infrared photon in the range 1000–2400 cm^{-1} has to be sufficient to cause the dissociation of the target ion. If the photon energy absorbed in a vibrational transition is around the binding energy of a solvent CO_2 molecule (which ranges from 15 to 25 kJ mol^{-1} or from 1250 to 2100 cm^{-1}) or greater, photodissociation can occur. Even for photon energies somewhat below the solvent binding energy, the energy content of the cluster prior to excitation (which is estimated to be of the same order of magnitude as the solvent binding energy[49,53]) will be sufficient to lead to the loss of a weakly bound CO_2 molecule from the cluster. As a consequence, the spectrum at cluster size y can be best understood as a probe of the structure of ions with size $(y - 1)$.

In this experiment, the smallest cluster ions for which photofragments were observed have the composition $[Ti(CO_2)_4]^-$. Since the detection scheme of our experiment relies on the presence of weakly bound CO_2 molecules, the absence of photofragmentation for $y \leq 3$ implies that the first three CO_2 units are strongly bound to the metal.

The infrared photodissociation spectra for $[Ti(CO_2)_y]^-$ anionic clusters are shown in Figure 1, with increasing numbers

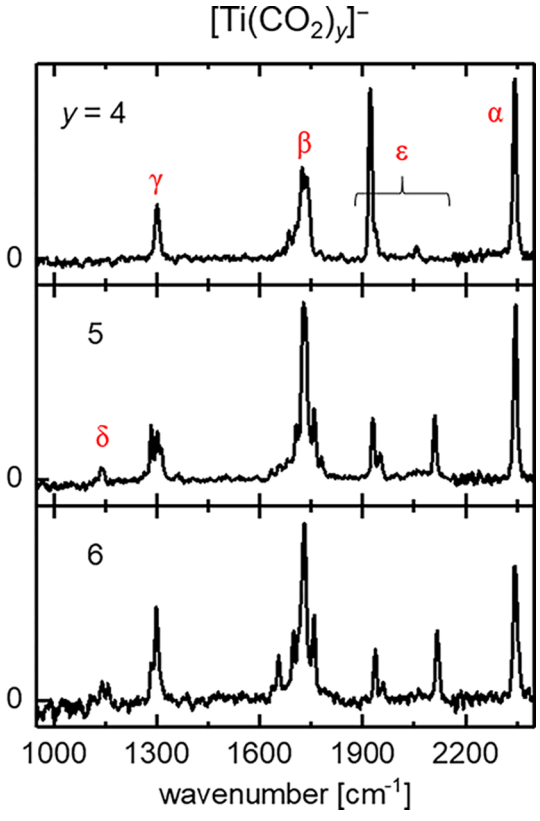

Figure 1. Infrared photodissociation spectra of $[Ti(CO_2)_y]^-$ (y = 4–6). Spectral regions of interest are indicated by Greek letters (see also Table 1).

DOI: 10.1021/acs.jpca.8b01843
J. Phys. Chem. A 2018, 122, 2983−2991

of CO_2 units ($y = 4-6$) interacting with a single titanium atom. The spectra consist of several distinct regions, labeled with Greek letters $\alpha-\varepsilon$, which are listed in Table 1. The spectra have some common intense features, which have been observed for specific types of ligands in other $[M(CO_2)_n]^-$ clusters.[54] In Table 1, we assign ligand vibrational modes that are likely to contribute to the absorption features in this region, based on past work[42−50] as well as computational results from the present work. Spectroscopic signatures of solvent CO_2 molecules are expected to occur in the range 2300−2350 cm^{-1}, while core ion signatures are found at lower wavenumbers.

Table 1. Observed Vibrational Peaks and Assignments for the Infrared Photodissociation Spectra of $[Ti(CO_2)_y]^-$ (y = 4−6)

feature	center ν (cm^{-1})	assignments
α	2340	antisymmetric CO_2 stretching mode of solvent CO_2
β	1730	asymmetric stretching mode of an η^2-(C,O) CO_2 ligand
		in-phase and out-of-phase combinations of free CO stretching vibrations of an oxalato ligand
		free CO stretching mode of an η^2-carbonato ligand
γ	1300	in-phase combination of metal-bound CO stretching motions in an oxalato ligand
δ	1140[a]	metal-bound CO stretching motions of a carbonato ligand
ε	1850−2200	metal-bound carbonyl stretching mode

[a]Feature δ grows in starting in at cluster size y = 5.

Some of the spectral regions, like β, are ambiguous regarding an assignment of spectral features to specific ligands, and even the combination of regions $\alpha-\delta$ cannot be used to clearly identify core ion structures. However, region ε contains features that can be uniquely assigned to carbonyl stretching vibrations. In addition to being clear evidence for Ti insertion into CO bonds of CO_2, we will show below that this region is the key to obtaining more detailed information on the cluster structure, in comparison with our computational results. It is particularly useful to note that we observe intense features in this region, compared to other spectral signatures, indicating the high abundance of carbonyl-containing core ions.

All structures reported here have doublet spin. Similar to Fe−CO_2 cluster anions,[49] we cannot rule out the presence of other spin states a priori. Our calculations find that the important structural isomers are minimum energy structures in both the doublet and the quartet states, and we cannot exclude the quartet states based on their predicted infrared spectra. However, the quartet states are more than 200 kJ mol^{-1} higher in energy than the doublet states. This is unusually high, compared to the difference between different spin states in other metal−CO_2 cluster anions, and we assume that the clusters are in doublet states based on this large energy difference.

As mentioned above, the observed spectrum for $[Ti(CO_2)_4]^-$ in the core ion region contains the spectroscopic signatures of a core ion with three CO_2 units bound to the Ti atom. We identify three low-lying core ion structures with the stoichiometry $[Ti(CO_2)_3]^-$ (Figure 2, III-A, III−B, and III−C) using quantum chemical calculations. Cluster structures are from here on labeled by the number of CO_2 units present in the cluster (Roman numerals), the core ion that cluster is based upon (capital letters), and if there are solvent CO_2 molecules parenthetical lowercase letters to distinguish different solvent positions (see also Supporting Information).

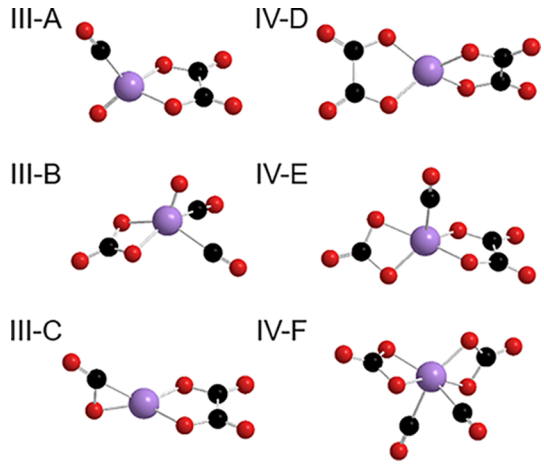

Figure 2. Core ion structures of $[Ti(CO_2)_y]^-$ (y = 3, 4) identified in this work. Ti atoms are shown in purple, C in black, and O in red.

Core ion A, represented by structure III-A, consists of three CO_2 units, two of which form an oxalato ligand, while the third CO_2 unit dissociates into an oxo and a carbonyl ligand upon insertion of the Ti atom into one of its CO bonds, resulting in a structure with C_s symmetry (the σ plane is formed by the O−Ti−CO plane). Core ion B (structure III−B) features a carbonato ligand, two carbonyl ligands, and an oxo ligand. This core ion also has C_s symmetry, with the σ plane bisecting the two carbonyl ligands. The third core ion structure, core ion C (structure III−C), unlike the other core ions, does not feature a CO ligand. Instead, one CO_2 unit binds to titanium in a bidentate η^2-(C,O) fashion (this ligand defines the σ plane of this C_s core ion), with two other CO_2 units forming an oxalato ligand. Solvation of these three core ions by a single CO_2 solvent molecule results in $[Ti(CO_2)_4]^-$ clusters (labeled IV-A, IV−B, and IV−C with varying solvent positions) whose signatures may be present in the experimental spectrum collected for $[Ti(CO_2)_4]^-$.

We note that several isomers of $[Ti(CO_2)_4]^-$ clusters exist with core ions containing four CO_2 units. These isomers have energies that are lower than or comparable to those of the low-energy solvated core ions (structures IV-D, IV-E, and IV−F in Figure 2 and others, see Supporting Information). However, as mentioned above, our experiment is not sensitive to their presence at this cluster size, since absorption of a single infrared photon will not result in dissociation without a weakly bound solvent molecule. While the cluster ions that give rise to the observed spectrum are not the lowest energy isomers for this cluster size, isomers other than the global minimum structure can be kinetically trapped during cluster formation, as has been shown for other $[M(CO_2)_n]^-$ clusters.[49,50] The relative energies of relevant structures are summarized in Table 2.

All core ions have high degrees of coordination—containing at least four bonds between the metal center and its ligands—consistent with the fact that no photodissociation signal was observed in experiments targeting smaller cluster sizes. As mentioned above, the high intensities of the carbonyl features relative to the signatures around 1700 cm^{-1} indicate that carbonyl-containing core ions clearly dominate the core ion structures with three CO_2 units. The signatures of the carbonyl

DOI: 10.1021/acs.jpca.8b01843
J. Phys. Chem. A 2018, 122, 2983−2991

Table 2. Calculated Relative Energies[a] of Isomers for $y = 4$ and 5

structure	energy (kJ mol^{-1})
$[Ti(CO_2)_4]^-$ relative energies	
IV-A(a)	0
IV-A(b)	5
IV-A(c)	10
IV-B(a)	37
IV-B(b)	44
IV-C(a)	72
IV-C(b)	78
IV-D	(−69)
IV-E	(−34)
IV-F	(6)
$[Ti(CO_2)_5]^-$ relative energies	
V-A(a)	71
V-A(b)	76
V-B(a)	108
V-C(a)	145
V-C(b)	150
V-D(a)	0
V-D(b)	5
V-E(a)	35
V-E(b)	37
V-E(c)	37
V-F(a)	77
V-F(b)	95

[a]Energies are given relative to the lowest energy isomer with at least one solvent molecule. Energies for other isomers, which cannot be experimentally observed, are listed in parentheses (see text). The structures for all listed isomers are shown in Supporting Information.

groups present in most of the calculated core ions are distinct and will be used to assign the infrared photodissociation spectra to contributing core ion structures.

Shown in Figure 3 is the experimental spectrum for $[Ti(CO_2)_4]^-$ compared to the calculated infrared spectra for core ions A, B, and C, solvated by a single solvent CO_2 molecule. The absorption features in regions α, β, γ, and ε are all well described by predicted vibrational modes in the three proposed core ion structures.[55,56] We note that there are no spectral features that are unique signatures of core isomer C, since features α, β, and γ are also predicted to occur for core isomer A, and there is no unambiguous proof that core ion C is contributing to the experimental spectrum. In fact, we will argue later in this paper that it is unlikely that core isomer C is significantly populated in the experiment.

The carbonyl stretching region for the smallest cluster size studied here, $[Ti(CO_2)_4]^-$, is shown in Figure 4, compared to calculated spectra of carbonyl-containing core ions relevant to this cluster size. The experimental spectrum contains three features in this region. The first peak, which is the most intense, appears at 1922 cm^{-1}. A shoulder appears just to the blue of this peak, at 1940 cm^{-1}. Finally, a small peak appears at 2056 cm^{-1}. The solvated core ions featuring carbonyl ligands (IV-A and IV−B in Figure 2) have distinct CO stretching signatures.

The lowest lying conformation of a solvated core ion with three CO_2 units is based on core ion A (structure IV-A(a)) The corresponding spectrum is shown in Figure 4b; its carbonyl stretching frequency is predicted at 1938 cm^{-1}. This conformation represents the lowest energy isomer for $y = 4$ with at least one solvent molecule, and isomer energies

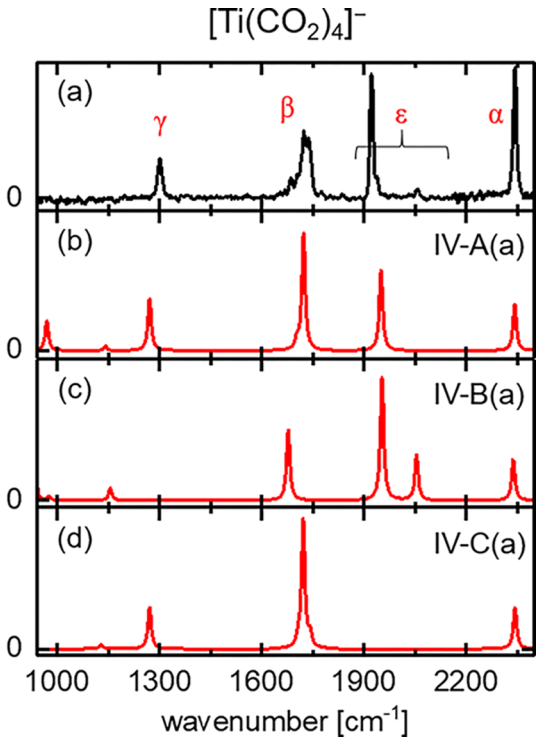

Figure 3. Experimental spectrum of $[Ti(CO_2)_4]^-$ (a) and computed spectra for several core ion isomers at this cluster size (b--d). Spectral regions of interest are indicated by Greek letters.

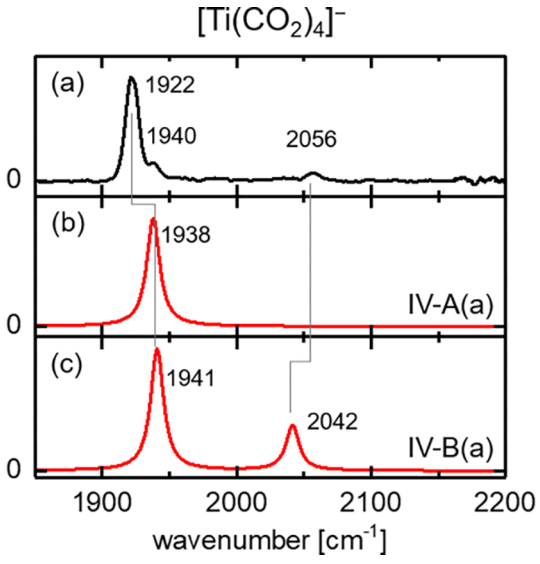

Figure 4. Carbonyl stretching region for $[Ti(CO_2)_4]^-$ showing (a) experimental and computed spectra for (b) structure IV-A(a) and (c) structure IV−B(a). Computed CO vibrational frequencies have been scaled by 0.9694. Numbers in each trace designate the band centers.

reported for all structures with this cluster size are given relative to this isomer. Other solvent conformers for core ion A (e.g., structures IV-A(b) and IV-A(c), see Supporting Information) have calculated zero-point-corrected energies up to 10 kJ mol^{-1} above the lowest energy form. Core ion A can be solvated by CO_2 in several positions (see Supporting Information, structures IV-A(a), IV-A(b), and IV-A(c)). The binding energies for the solvent CO_2 depend on its position and are calculated to be in the range 15−25 kJ mol^{-1} (1300−2100

DOI: 10.1021/acs.jpca.8b01843
J. Phys. Chem. A 2018, 122, 2983−2991

cm^{-1}) for this core ion, enabling photodissociation by infrared photons without significant suppression of core ion features in the carbonyl stretching region. The position of the solvent molecule does not significantly change the calculated CO stretching mode, as all calculated frequencies for solvated core ions of family A range from 1934 to 1939 cm^{-1}, and we assign this mode to the high-intensity feature at 1922 cm^{-1}.

Similar to the arguments presented for core ion isomer A, solvated core ion B can also be accessed experimentally in the spectrum for $y = 4$. This core ion, which features two carbonyl ligands, is solvated preferentially at the carbonato ligand. Solvation of core ion B results in cluster structures that are at least 37 kJ mol^{-1} higher in energy than the lowest energy solvent conformer of core ion A. The calculated binding energy of the CO_2 solvent molecule is slightly larger (19−26 kJ mol^{-1}, 1600−2200 cm^{-1}) than for core ion A, but we can still expect photodissociation to occur in the carbonyl stretching region with little to no suppression. Comparing the experimental spectrum with the calculated carbonyl stretching signatures of this cluster, we see that there is some evidence for the appearance of solvated core ion B (Figure 4c). With two equivalent carbonyl ligands, this core ion has two coupled CO oscillators that give rise to two vibrational features—the in-phase and out-of-phase combinations of the two CO stretching oscillations. The higher intensity out-of-phase feature is predicted at 1941 cm^{-1}, close to the shoulder on the intense CO stretching feature in the experimental spectrum, and the in-phase combination (calculated 2042 cm^{-1}) is close to the small feature observed experimentally at 2056 cm^{-1}. On the basis of the predicted intensity ratio of the two modes, we assign the out-of-phase mode to the shoulder at 1940 cm^{-1} and the in-phase mode to the peak at 2056 cm^{-1}.

With increasing degree of solvation, the experimentally observed vibrational modes in the carbonyl stretching region blue shift by ca. 7 cm^{-1} per solvent molecule. We performed calculations on clusters with $y = 5$, which exhibit 5−10 cm^{-1} blue shifts compared to $y = 4$, depending on the solvent positions, consistent with the experiment. Due to the computational cost, the increasing number of possible solvation isomers, and the fact that there is no significant change in the infrared spectrum from $y = 5$ to $y = 6$, we did not perform calculations on clusters with $y > 5$. The most notable difference between the experimental spectra for $y = 4$ and $y = 5$ and 6 is the significant intensity increase in the peak close to 2100 cm^{-1} relative to the peak appearing ca. 1930 cm^{-1}, resulting in similar intensities of the two peaks.

At clusters with $y > 4$, larger core ions may come into play. Core ions D−F, shown in Figure 2, contain four CO_2 units (see Table 2 for relative energies). Structure V-D(a) is the lowest energy isomer of all structures containing five CO_2 units and is 71 kJ mol^{-1} lower in energy than structure V-A(a). Core ion D does not contain any carbonyl ligands; instead, it features two bidentate oxalato ligands. This structure is similar to the structure recently observed in $[Mn(CO_2)_n]^-$ clusters.[50] This core ion likely contributes to the $[Ti(CO_2)_y]$ ($y = 5$ and 6) experimental spectra with intensity in regions β and γ (Figure 1).

Core ions E and F have at least one carbonyl ligand. In core ion E, two of the CO_2 units form an oxalato ligand while the other two form a carbonato ligand and a carbonyl ligand. Solvated structure V-E(a) lies 37 kJ mol^{-1} lower in energy than V-A(a). Core ion F has C_2 symmetry, with two carbonato and two carbonyl ligands. Structure V−F(a) is nearly isoenergetic with V-A(a), lying just 6 kJ mol^{-1} higher in energy. Several other higher energy core ions were identified computationally, including carbonyl-containing core ions G and H that are within 40 kJ mol^{-1} of the energy of V-A(a) (Supporting Information). However, these structures either have only weakly bound CO ligands (ca. 7 kJ mol^{-1}) which are unlikely to survive the exothermic insertion reactions leading to their formation. Others are significantly higher in energy (>40 kJ mol^{-1}) than V-A(a); all structures are listed in the Supporting Information.

Solvation of core ions D−F results in weakly bound CO_2 solvent molecules, enabling us to observe these core ions in the $[Ti(CO_2)_y]^-$ ($y = 5$ and 6) spectra. The binding energy for CO_2 solvent molecules on these core ions is 16−21 kJ mol^{-1} for core ion D, 19−22 kJ mol^{-1} for core ion E, and ca. 19 kJ mol^{-1} for core ion F. The simulated spectra for structures V-A(a)−V-F(a) for the $y = 5$ cluster are shown in Figure 5 along with the experimental $[Ti(CO_2)_5]^-$ spectrum. The peaks at 1930 and 1951 cm^{-1} in the experimental spectrum are assigned to solvated core ions A and B. On the basis of the fact that core

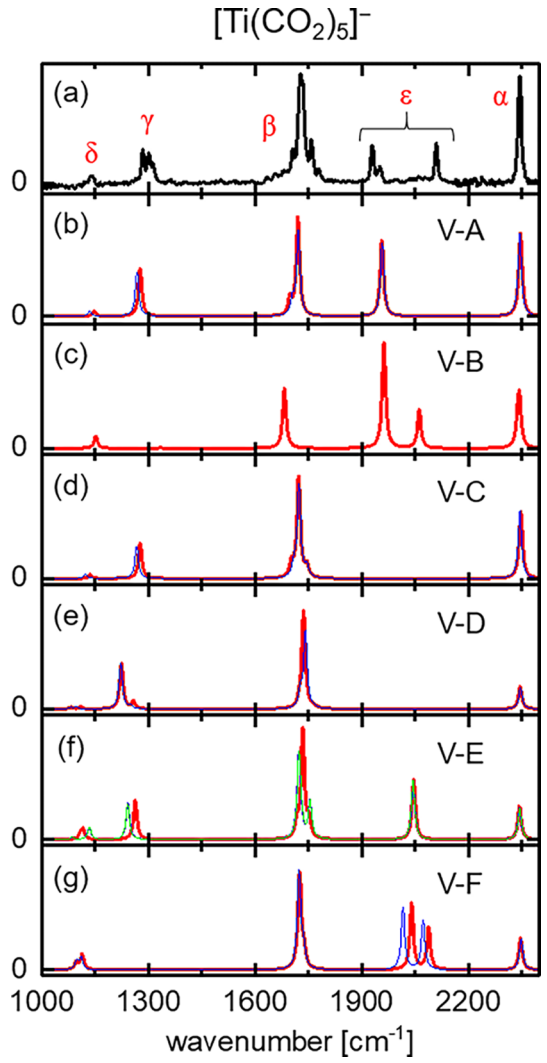

Figure 5. Experimental spectrum of $[Ti(CO_2)_5]^-$ (a) and computed spectra for several core ion isomers at this cluster size (b−g). Traces with different colors in the computed spectra correspond to different solvent positions. Spectral regions of interest are indicated by Greek letters.

DOI: 10.1021/acs.jpca.8b01843
J. Phys. Chem. A 2018, 122, 2983−2991

ion V-E leads to the lowest energy carbonyl-containing cluster isomers at this cluster size, we tentatively assign the feature at 2110 cm^{-1} to core ion E. The broad, low-intensity signal centered on 2050 cm^{-1} is tentatively assigned to the two carbonyl modes in V−F. These modes depend on the solvent conformation for this core ion (see Figure 5g). At the same time, the OC−Ti−CO bending vibration is very soft (unscaled predicted value at 47.65 cm^{-1}), and we expect it to be excited in the ions prior to irradiation, which likely leads to considerable broadening. Core ions E and F both contain carbonato ligands. Since these core ions are all expected to begin contributing to experimental spectra for $y > 5$, our assignments are consistent with the increasing relative intensity in region δ (Figures 1 and 5 and Table 1).

While core ion D constitutes the lowest energy isomer for all clusters with $y \geq 4$, it is important to note that insertion structures are still important for all cluster sizes discussed in the present work. Their importance can be gauged by comparing the relative intensities of the spectral regions β and ε (see Figure 5). All calculated structures contribute to region β, through η^2-(C,O), oxalato, or carbonato ligands, and the predicted wavenumbers are very close, consistent with the substructure and width of feature β. In contrast, the features belonging to carbonyl stretching modes are spread out over a much larger spectral region. The fact that the integrated intensity over the carbonyl region is similar to that of region β indicates that carbonyl-containing core ions are still important species at larger cluster sizes, even though they are not lowest in energy. To illustrate the fact that bond insertion isomers are important species, even for $y \geq 4$, Figure 6 shows a simulation

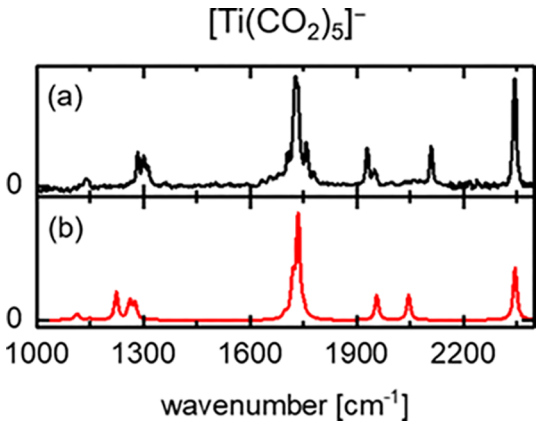

Figure 6. Comparison of the experimental $[Ti(CO_2)_5]^-$ spectrum (a) with the sum of the calculated spectra (b) for isomers V-A, V-D, and V-E.

for a hypothetical isomer mixture, where the predicted spectra for isomers V-A(a), V-D(a), and V-E(a) (as shown in Figure 5) have been added with equal weight. Comparison of the simulation for this mixture of isomers with the experimental spectrum shows that a very similar overall band pattern is achieved, with similar relative intensities as those observed experimentally. The comparison demonstrates that insertion structures are at least as important as the lowest energy isomer V-D(a) in the isomer mixture of the ion beam, evidenced by the 2:1 ratio for the abundance of insertion vs noninsertion isomers in the simulation.

Insertion of Ti into CO Bonds. The appearance of intense features characteristic of carbonyl groups shows that bond insertion is an important reaction during the formation of $[Ti(CO_2)_y]^-$ clusters. Each CO ligand is formed upon insertion of the metal atom into the carbon−oxygen bond of a CO_2 molecule, simultaneously forming an oxo ligand. Bond dissociation could in principle occur in the laser vaporization plasma (the bond dissociation energy of free CO_2 is 532.2 kJ mol^{-1}).[57] However, while some insertion-type structures have been previously predicted as global minimum structures for $[M(CO_2)_n]^-$ cluster anions (M = Cu, Co, Ni), only weak experimental evidence exists for their formation in experiments under similar conditions as in the present work.[44−46] Only in the case of $[Fe(CO_2)_n]^-$ anionic clusters did we positively identify the formation of structures containing a CO ligand.[49] Bond insertion has been observed for $[Ti(CO_2)_n]^+$ cations,[30] and similarly, for titanium−CO_2 cluster anions, we can unambiguously assign the features in the carbonyl stretching region as vibrations of CO ligands bound to a titanium atom, formed by an insertion process.

Of course, there are other possible core ion structures that do not exhibit a carbonyl ligand, and it is a fair question whether the carbonyl-containing species are the dominant species in clusters where many different and in some cases lower energy isomers may be populated. There are two key pieces of evidence that imply that bond insertion processes are indeed dominating core ion formation in $[Ti(CO_2)_y]^-$ clusters.

First, as mentioned above, comparing the predicted intensities of infrared signatures around 1700 cm^{-1} that are common to most CO_2 based ligands with the predicted intensities in the carbonyl stretching region, one would expect that a large abundance of species without carbonyl ligands would lead to an aggregate feature in region β that would dwarf the signatures in the carbonyl region. The experimental spectra and the simulation presented in Figure 6 show that this is not the case.

Second, a computational treatment of Ti insertion into a C−O bond on CO_2 suggests that we should expect this process to be much more efficient than for later first-row transition metals, as we will show in the following paragraphs.

To investigate the potential energy landscape of titanium anion insertion into the C−O bond of a CO_2 molecule, we simulated this process by scanning one of the C−O bond distances of a CO_2 molecule in the presence of a bare metal atom M and an excess electron (Figure 7a), relaxing all other coordinates. For M = Ti, short C−O bond distances result in the formation of the local minimum bidentate η^2-(C,O) structure of $[TiCO_2]^-$ (Figure 7a). However, only a small barrier (ca. 27 kJ mol^{-1}) separates the η^2-(C,O) structure from the global minimum insertion structure ($OTiCO^-$), which lies ca. 68 kJ mol^{-1} lower in energy compared to the bidentate structure. Compared with later first-row transition metals, the barrier to formation of a carbonyl ligand is very small for titanium. Recently, we reported a barrier of more than 100 kJ mol^{-1} for Fe insertion into the C−O bond of CO_2 in an $[Fe(OCO)]^-$ complex.[49] Even more substantial barriers exist for other metals, e.g., ca. 200 kJ mol^{-1} for the analogous Ni complex (Figure 7a, blue circles). In the case of titanium−CO_2 interaction, C−O bond breaking occurs readily, and the required energy can easily be supplied in the ion source, even by mere condensation of CO_2 onto the metal atom. These results are reminiscent of the observed bond insertion processes that occur for neutral Ti atoms.[22,24,26] Because of the high oxophilicity of titanium, the metal−oxygen bond formed upon bond insertion (forming the metal−oxo ligand) is stronger than

DOI: 10.1021/acs.jpca.8b01843
J. Phys. Chem. A 2018, 122, 2983−2991

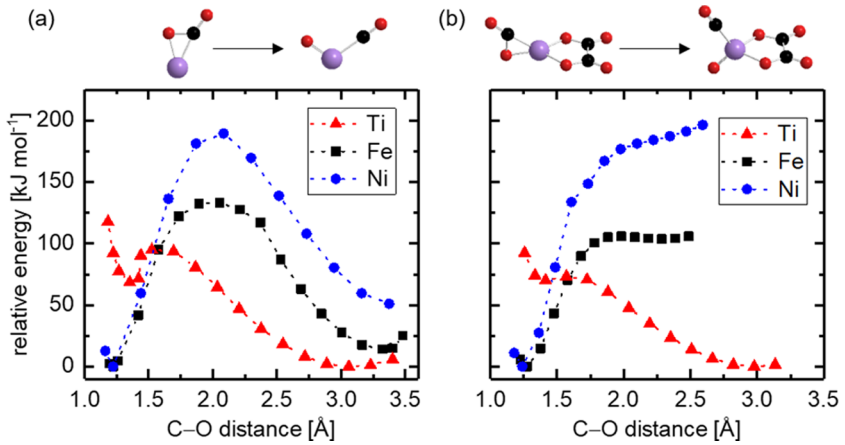

Figure 7. Barriers to metal atom insertion into a C−O bond in $[M(CO_2)_y]^-$ (M = Ti, Fe, Ni) for (a) insertion by the bare metal and (b) insertion by a metal atom chelated by an oxalato ligand. Energies are relative to the minimum energy structure in each case.

the same bond formed for other metals. The calculated Mulliken−Mayer bond orders for the M−O bond in each case are as follows: Ti, 2.11; Fe, 1.52; Ni, 1.29, following the oxophilicity trend of Ti > Fe > Ni.[58] This is reflected in the analogous potential energy curves for bond insertion of Fe or Ni (Figure 7a), where insertion is associated with a much higher barrier, and the energies for the inserted metal and the η^2-(C,O) structure are similar.

Schwarz and co-workers showed that the presence of certain ligands makes C−O bond insertion more favorable in cationic titanium hydrides.[59,60] We similarly note the impact of a ligand on C−O bond insertion. Figure 7b shows the results of scanning the C−O bond distance of a CO_2 molecule in the presence of a $M(CO_2)_2^-$ species with two CO_2 units forming an oxalato ligand. Similar to the scenario without the oxalato ligand, the CO_2 first binds to the titanium metal center in a bidentate binding scheme (η^2-(C,O)), forming core ion C (structure III−C). While there is again a small barrier between this core ion and the metal-inserted structure, the presence of the oxalato ligand brings the barrier down to less than 5 kJ mol^{-1}. The resulting metal insertion structure is in fact core ion A (structure III-A), which is 72 kJ mol^{-1} lower in energy than core ion C. Due to the very small barrier, core ion C will likely be converted to core ion A. We therefore assume that core ion C does not contribute significantly to the observed signatures in our experimental spectra. Again, Ti behaves differently from Fe and Ni, where an oxalato ligand raises the energy of the inserted structure (Figure 7b). While insertion structures have been positively identified for $[Fe(CO_2)_n]^-$ cluster anions, they appeared in conjunction with carbonato ligands, not oxalato ligands.

Finally, we note that the overall charge in the complex plays an important role for the chemistry in titanium−CO_2 clusters. Zhou and co-workers[30] performed IR photodissociation spectroscopy on titanium−CO_2 cluster cations. While they also find bond insertion structures to dominate the composition of their ion beam, all other CO_2 units in their simulated structures are bound by electrostatic interaction, forming OCO···Ti^+ structures, similar to those found by the Duncan and Mckenzie groups for other metal−CO_2 cluster cations.[31,32,61−65] In contrast, titanium−CO_2 cluster anions form very different metal−organic complexes, where strong metal−oxygen bonds are formed, and carbonato as well as oxalato ligands result from the interaction of several CO_2 units in the presence of the metal atom and the excess electron.[42−50]

Considering the charge distribution in cluster ions, anionic complexes display a very rich electronic structure where the traditional concepts of formal charges are mostly too simplistic to reflect the electronic structure of the complex in any reasonable approximation. For example, the Ti atom has a partial charge close to +1 e in the presence of a carbonato ligand (isomers III−B and IV−B), but in the presence of an oxalato ligand (isomer III-A and IV-A), the partial charge is ca. +1.4 e. For the global minimum at $y = 4$, which has two oxalato ligands (isomer IV-D), the partial charge on the Ti atom is ca. +1.7 e. Overall, the partial charge on the Ti atom seems to be dominated by the identity of the ligands, where oxalato ligands will accumulate ca. −1.4 e and carbonato ligands have ca. −1.2 e. Neither of these partial charges are properly described by the expected formal charge of −2 e for these ligands. Similar to other metal−CO_2 cluster anions, the chemistry displayed by Ti−CO_2 cluster anions is much richer than that of most of their cationic counterparts.

CONCLUSIONS

The results of spectroscopic studies of $[Ti(CO_2)_y]^-$ anionic clusters in vacuo demonstrate the strong tendency for C−O bond insertion by titanium in anionic complexes with CO_2. Through observation of the metal carbonyl CO stretch region in infrared photodissociation spectra and supported by quantum chemical calculations, we identify products of titanium insertion. The calculated barrier to bond breaking is small in these complexes, and the bond insertion process is assisted by the presence of an oxalato ligand. The oxo groups produced by bond insertion can combine with additional CO_2 molecules to form carbonato ligands. Overall, reactions of Ti atoms with CO_2 in the presence of an excess electron result in the formation of oxalato, carbonato, carbonyl, and oxo ligands. These results are consistent with the observation of oxalate, carbonate/bicarbonate, and CO products at Ti catalyst sites in condensed phase catalysts.

ASSOCIATED CONTENT

Supporting Information

The Supporting Information is available free of charge on the ACS Publications website at DOI: 10.1021/acs.jpca.8b01843.

DOI: 10.1021/acs.jpca.8b01843
J. Phys. Chem. A 2018, 122, 2983−2991

Simulated spectra for $[Ti(CO_2)_3]^-$ clusters, and calculated geometries and vibrational frequencies of all structures (PDF)

AUTHOR INFORMATION

Corresponding Author

*E-mail: weberjm@jila.colorado.edu.

ORCID

Leah G. Dodson: 0000-0001-5960-056X

J. Mathias Weber: 0000-0002-5493-5886

Notes

The authors declare no competing financial interest.

ACKNOWLEDGMENTS

We gratefully acknowledge funding from the National Science Foundation (NSF) through the NSF AMO Physics Frontier Center at JILA (PHY-1125844 and PHY-1734006). We also acknowledge graduate student support from the U.S. Department of Education through a GAANN Fellowship for M.C.T. This research was performed while L.G.D. held an NRC Research Associateship award at NIST.

REFERENCES

(1) Lee, J.; Sorescu, D. C.; Deng, X. Electron-Induced Dissociation of CO_2 on TiO_2(110). *J. Am. Chem. Soc.* **2011**, *133*, 10066−10069.

(2) Tan, S.; Zhao, Y.; Zhao, J.; Wang, Z.; Ma, C.; Zhao, A.; Wang, B.; Luo, Y.; Yang, J.; Hou, J. CO_2 Dissociation Activated Through Electron Attachment on the Reduced Rutile TiO_2(110)-1 × 1 Surface. *Phys. Rev. B: Condens. Matter Mater. Phys.* **2011**, *84*, 155418.

(3) Anpo, M. Photocatalytic Reduction of CO_2 with H_2O on Highly Dispersed Ti-oxide Catalysts as a Model of Artificial Photosynthesis. *J. CO2 Util.* **2013**, *1*, 8−17.

(4) Wang, G.; Su, J.; Gong, Y.; Zhou, M.; Li, J. Chemistry on Single Atoms: Spontaneous Hydrogen Production from Reactions of Transition-Metal Atoms with Methanol at Cryogenic Temperatures. *Angew. Chem., Int. Ed.* **2010**, *49*, 1302−1305.

(5) Samantaray, M. K.; Kavitake, S.; Morlanés, N.; Abou-Hamad, E.; Hamieh, A.; Dey, R.; Basset, J.-M. Unearthing a Well-Defined Highly Active Bimetallic W/Ti Precatalyst Anchored on a Single Silica Surface for Metathesis of Propane. *J. Am. Chem. Soc.* **2017**, *139*, 3522−3527.

(6) Nanayakkara, C. E.; Larish, W. A.; Grassian, V. H. Titanium Dioxide Nanoparticle Surface Reactivity with Atmospheric Gases, CO_2, SO_2, and NO_2: Roles of Surface Hydroxyl Groups and Adsorbed Water in the Formation and Stability of Adsorbed Products. *J. Phys. Chem. C* **2014**, *118*, 23011−23021.

(7) Baltrusaitis, J.; Schuttlefield, J.; Zeitler, E.; Grassian, V. H. Carbon Dioxide Adsorption on Oxide Nanoparticle Surfaces. *Chem. Eng. J.* **2011**, *170*, 471−481.

(8) Martra, G. Lewis Acid and Base Sites at the Surface of Microcrystalline TiO_2 Anatase: Relationships Between Surface Morphology and Chemical Behaviour. *Appl. Catal., A* **2000**, *200*, 275−285.

(9) Liao, L. F.; Lien, C. F.; Shieh, D. L.; Chen, M. T.; Lin, J. L. FTIR Study of Adsorption and Photoassisted Oxygen Isotopic Exchange of Carbon Monoxide, Carbon Dioxide, Carbonate, and Formate on TiO_2. *J. Phys. Chem. B* **2002**, *106*, 11240−11245.

(10) Su, W.; Zhang, J.; Feng, Z.; Chen, T.; Ying, P.; Li, C. Surface Phases of TiO_2 Nanoparticles Studied by UV Raman Spectroscopy and FT-IR Spectroscopy. *J. Phys. Chem. C* **2008**, *112*, 7710−7716.

(11) Böhme, D. K.; Schwarz, H. Gas-Phase Catalysis by Atomic and Cluster Metal Ions: The Ultimate Single-Site Catalysts. *Angew. Chem., Int. Ed.* **2005**, *44*, 2336−2354.

(12) Dossmann Soldi-Lose, H.; Afonso, C.; Lesage, D.; Tabet, J.-C.; Uggerud, E. Formation and Characterization of Gaseous Adducts of Carbon Dioxide to Magnesium, $(CO_2)MgX-$ (X = OH, Cl, Br). *Angew. Chem., Int. Ed.* **2012**, *51*, 6938−6941.

(13) O'Hair, R. A. J.; Rijs, N. J. Gas Phase Studies of the Pesci Decarboxylation Reaction: Synthesis, Structure, and Unimolecular and Bimolecular Reactivity of Organometallic Ions. *Acc. Chem. Res.* **2015**, *48*, 329−340.

(14) Brathwaite, A. D.; Duncan, M. A. Infrared Photodissociation Spectroscopy of Saturated Group IV (Ti, Zr, Hf) Metal Carbonyl Cations. *J. Phys. Chem. A* **2013**, *117*, 11695−11703.

(15) Gentleman, A. S.; Green, A. E.; Price, D. R.; Cunningham, E. M.; Iskra, A.; Mackenzie, S. R. Infrared Spectroscopy of $Au^+(CH_4)_n$ Complexes and Vibrationally-Enhanced C−H Activation Reactions. *Top. Catal.* **2017**.10.1007/s11244-017-0868-z

(16) Hermes, A. C.; Hamilton, S. M.; Cooper, G. A.; Kerpal, C.; Harding, D. J.; Meijer, G.; Fielicke, A.; Mackenzie, S. R. Infrared Driven CO Oxidation Reactions on Isolated Platinum Cluster Oxides, $Pt_nO_m^+$. *Faraday Discuss.* **2012**, *157*, 213−225.

(17) Miller, G. B. S.; Esser, T. K.; Knorke, H.; Gewinner, S.; Schöllkopf, W.; Heine, N.; Asmis, K. R.; Uggerud, E. Spectroscopic Identification of a Bidentate Binding Motif in the Anionic Magnesium−CO_2 Complex ($[ClMgCO_2]^-$). *Angew. Chem., Int. Ed.* **2014**, *53*, 14407−14410.

(18) Mascetti, J.; Tranquille, M. Fourier Transform Infrared Studies of Atomic Titanium, Vanadium, Chromium, Iron, Cobalt, Nickel and Copper Reactions with Carbon Dioxide in Low-Temperature Matrices. *J. Phys. Chem.* **1988**, *92*, 2177−2184.

(19) Jeung, G. H. Activation of CO_2 Coordinated to a Ti Atom. *Mol. Phys.* **1989**, *67*, 747−756.

(20) Jeung, G.-H. Theoretical Study on Coordination of CO_2 to Third Row Metal Atoms (Ca−Mn, Cu, Zn). *Chem. Phys. Lett.* **1995**, *232*, 319−327.

(21) Chertihin, G. V.; Andrews, L. Infrared Spectra of the Reaction Products of Laser-Ablated Titanium Atoms and Oxides with Carbon Monoxide in Solid Argon. *J. Am. Chem. Soc.* **1995**, *117*, 1595−1602.

(22) Pápai, I.; Mascetti, J.; Fournier, R. Theoretical Study of the Interaction of the Ti Atom with CO_2: Cleavage of the C−O Bond. *J. Phys. Chem. A* **1997**, *101*, 4465−4471.

(23) Zhou, M.; Andrews, L. Infrared Spectra and Density Functional Calculations for OMCO, $OM^-(\eta^2$-CO), $OMCO^+$, and $OMOC^+$ (M = V, Ti) in Solid Argon. *J. Phys. Chem. A* **1999**, *103*, 2066−2075.

(24) Mascetti, J.; Galan, F.; Pàpai, I. Carbon Dioxide Interaction with Metal Atoms: Matrix Isolation Spectroscopic Study and DFT Calculations. *Coord. Chem. Rev.* **1999**, *190-192*, 557−576.

(25) Zhuang, J.; Li, Z. H.; Fan, K.; Zhou, M. Matrix Isolation Spectroscopic and Theoretical Study of Carbon Dioxide Activation by Titanium Oxide Molecules. *J. Phys. Chem. A* **2012**, *116*, 3388−3395.

(26) Hwang, D.-Y.; Mebel, A. M. Ab Initio Study of the Reaction Mechanism of CO_2 with Ti Atom in the Ground and Excited Electronic States. *J. Chem. Phys.* **2002**, *116*, 5633−5642.

(27) Sodupe, M.; Branchadell, V.; Rosi, M.; Bauschlicher, C. W. Theoretical Study of $M^+−CO_2$ and OM^+CO Systems for First Transition Row Metal Atoms. *J. Phys. Chem. A* **1997**, *101*, 7854−7859.

(28) Koyanagi, G. K.; Bohme, D. K. Gas-Phase Reactions of Carbon Dioxide with Atomic Transition-Metal and Main-Group Cations: Room-Temperature Kinetics and Periodicities in Reactivity. *J. Phys. Chem. A* **2006**, *110*, 1232−1241.

(29) Walker, N. R.; Walters, R. S.; Duncan, M. A. Infrared Photodissociation Spectroscopy of $V^+(CO_2)_n$ and $V^+(CO_2)_nAr$ Complexes. *J. Chem. Phys.* **2004**, *120*, 10037−10045.

(30) Xing, X. P.; Wang, G. J.; Wang, C. X.; Zhou, M. F. Infrared Photodissociation Spectroscopy of $Ti^+(CO_2)_2Ar$ and $Ti^+(CO_2)_n$ (*n* = 3−7) Complexes. *Chin. J. Chem. Phys.* **2013**, *26*, 687−687.

(31) Walker, N. R.; Grieves, G. A.; Walters, R. S.; Duncan, M. A. The Metal Coordination in $Ni^+(CO_2)_n$ and $NiO_2^+(CO_2)_m$ Complexes. *Chem. Phys. Lett.* **2003**, *380*, 230−236.

(32) Walker, N. R.; Walters, R. S.; Grieves, G. A.; Duncan, M. A. Growth Dynamics and Intracluster Reactions in $Ni^+(CO_2)_n$ Complexes via Infrared Spectroscopy. *J. Chem. Phys.* **2004**, *121*, 10498−10507.

DOI: 10.1021/acs.jpca.8b01843
J. Phys. Chem. A 2018, 122, 2983−2991

(33) Jaeger, J. B.; Jaeger, T. D.; Brinkmann, N. R.; Schaefer, H. F.; Duncan, M. A. Infrared Photodissociation Spectroscopy of $Si^+(CO_2)_n$ and $Si^+(CO_2)_nAr$ Complexes - Evidence for Unanticipated Intracluster Reactions. *Can. J. Chem.* **2004**, *82*, 934−946.
(34) Weber, J. M. A Pulsed Ion Source for the Preparation of Metal Containing Cluster Anions using Supersonic Entrainment of Laser Vaporized Metal. *Rev. Sci. Instrum.* **2005**, *76*, 043301.
(35) Stoermer, C. W.; Gilb, S.; Friedrich, J.; Schooss, D.; Kappes, M. M. A High Resolution Dual Mass Gate for Ion Separation in Laser Desorption/Ionization Time of Flight Mass Spectrometry. *Rev. Sci. Instrum.* **1998**, *69*, 1661−1664.
(36) Riedel, J.; Yan, S.; Kawamata, H.; Liu, K. A Simple Yet Effective Multipass Reflector for Vibrational Excitation in Molecular Beams. *Rev. Sci. Instrum.* **2008**, *79*, 033105.
(37) Ahlrichs, R.; Bär, M.; Häser, M.; Horn, H.; Kölmel, C. Electronic Structure Calculations on Workstation Computers: The Program System TURBOMOLE. *Chem. Phys. Lett.* **1989**, *162*, 165−169.
(38) Becke, A. D. Density-Functional Exchange-Energy Approximation with Correct Asymptotic Behavior. *Phys. Rev. A: At., Mol., Opt. Phys.* **1988**, *38*, 3098−3100.
(39) Lee, C.; Yang, W.; Parr, R. G. Development of the Colle-Salvetti Correlation-Energy Formula into a Functional of the Electron Density. *Phys. Rev. B: Condens. Matter Mater. Phys.* **1988**, *37*, 785−789.
(40) Grimme, S. Semiempirical GGA-Type Density Functional Constructed with a Long-Range Dispersion Correction. *J. Comput. Chem.* **2006**, *27*, 1787−1799.
(41) Weigend, F.; Ahlrichs, R. Balanced Basis Sets of Split Valence, Triple Zeta Valence and Quadruple Zeta Valence Quality for H to Rn: Design and Assessment of Accuracy. *Phys. Chem. Chem. Phys.* **2005**, *7*, 3297−3305.
(42) Knurr, B. J.; Weber, J. M. Solvent-Driven Reductive Activation of Carbon Dioxide by Gold Anions. *J. Am. Chem. Soc.* **2012**, *134*, 18804−18808.
(43) Knurr, B. J.; Weber, J. M. Solvent-Mediated Reduction of Carbon Dioxide in Anionic Complexes with Silver Atoms. *J. Phys. Chem. A* **2013**, *117*, 10764−10771.
(44) Knurr, B. J.; Weber, J. M. Infrared Spectra and Structures of Anionic Complexes of Cobalt with Carbon Dioxide Ligands. *J. Phys. Chem. A* **2014**, *118*, 4056−4062.
(45) Knurr, B. J.; Weber, J. M. Interaction of Nickel with Carbon Dioxide in $[Ni(CO_2)_n]^-$ Clusters Studied by Infrared Spectroscopy. *J. Phys. Chem. A* **2014**, *118*, 8753−8757.
(46) Knurr, B. J.; Weber, J. M. Structural Diversity of Copper−CO_2 Complexes: Infrared Spectra and Structures of $[Cu(CO_2)_n]^-$ Clusters. *J. Phys. Chem. A* **2014**, *118*, 10246−10251.
(47) Knurr, B. J.; Weber, J. M. Structures of $[CoO(CO_2)_n]^-$ and $[NiO(CO_2)_n]^-$ Clusters Studied by Infrared Spectroscopy. *J. Phys. Chem. A* **2015**, *119*, 843−850.
(48) Thompson, M. C.; Ramsay, J.; Weber, J. M. Solvent-Driven Reductive Activation of CO_2 by Bismuth: Switching from Metalloformate Complexes to Oxalate Products. *Angew. Chem., Int. Ed.* **2016**, *55*, 15171−15174.
(49) Thompson, M. C.; Dodson, L. G.; Weber, J. M. Structural Motifs of $[Fe(CO_2)_n]^-$ Clusters. *J. Phys. Chem. A* **2017**, *121*, 4132−4138.
(50) Thompson, M. C.; Ramsay, J.; Weber, J. M. Interaction of CO_2 with Atomic Manganese in the Presence of an Excess Negative Charge Probed by Infrared Spectroscopy of $[Mn(CO_2)_n]^-$ Clusters. *J. Phys. Chem. A* **2017**, *121*, 7534−7542.
(51) Glendening, E. D.; Badenhoop, J. K.; Reed, A. E.; Carpenter, J. E.; Bohmann, J. A.; Morales, C. M.; Weinhold, F. *NBO 5.0*; Theoretical Chemistry Institute, University of Wisconsin: Madison, WI, 2001.
(52) Shao, Y.; Gan, Z.; Epifanovsky, E.; Gilbert, A. T. B.; Wormit, M.; Kussmann, J.; Lange, A. W.; Behn, A.; Deng, J.; Feng, X.; et al. Advances in Molecular Quantum Chemistry Contained in the Q-Chem 4 Program Package. *Mol. Phys.* **2015**, *113*, 184−215.
(53) Klots, C. E. Evaporative Cooling. *J. Chem. Phys.* **1985**, *83*, 5854−5860.
(54) Dodson, L. G.; Thompson, M. C.; Weber, J. M. Characterization of Intermediate Oxidation States in CO_2 Activation. *Annu. Rev. Phys. Chem.* **2018**, *69*, in press 10.1146/annurev-physchem-050317-021122.
(55) Huber, K. P.; Herzberg, G. *Molecular Spectra and Molecular Structure IV. Constants of Diatomic Molecules*; Springer Science +Business Media: New York, 1979.
(56) Irikura, K. K. Experimental Vibrational Zero-Point Energies: Diatomic Molecules. *J. Phys. Chem. Ref. Data* **2007**, *36*, 389−397.
(57) Darwent, B. d. *Bond Dissociation Energies in Simple Molecules*; United States Department of Commerce, National Bureau of Standards, 1970.
(58) Kepp, K. P. A Quantitative Scale of Oxophilicity and Thiophilicity. *Inorg. Chem.* **2016**, *55*, 9461−9470.
(59) Firouzbakht, M.; Zhou, S.; González-Navarrete, P.; Schlangen, M.; Kaupp, M.; Schwarz, H. Metal-Dependent Strengthening and Weakening of M−H and M−C Bonds by an Oxo Ligand: Thermal Gas-Phase Activation of Methane by $[OMH]^+$ and $[MH]^+$ (M = Mo, Ti). *Chem. - Eur. J.* **2017**, *23*, 12346−12352.
(60) Tang, S.-Y.; Rijs, N. J.; Li, J.; Schlangen, M.; Schwarz, H. Ligand-Controlled CO_2 Activation Mediated by Cationic Titanium Hydride Complexes, $[LTiH]^+$ (L = Cp_2, O. *Chem. - Eur. J.* **2015**, *21*, 8483−8490.
(61) Gregoire, G.; Duncan, M. A. Infrared Spectroscopy to Probe Structure and Growth Dynamics in Fe^+-$(CO_2)_n$ Clusters. *J. Chem. Phys.* **2002**, *117*, 2120−2130.
(62) Gregoire, G.; Velasquez, J.; Duncan, M. A. Infrared Photodissociation Spectroscopy of Small $Fe^+(CO_2)_n$ and $Fe^+(CO_2)_n$ Ar Clusters. *Chem. Phys. Lett.* **2001**, *349*, 451−457.
(63) Walters, R. S.; Brinkmann, N. R.; Schaefer, H. F.; Duncan, M. A. Infrared Photodissociation Spectroscopy of Mass-Selected $Al^+(CO_2)_n$ and $Al^+(CO_2)_nAr$ Clusters. *J. Phys. Chem. A* **2003**, *107*, 7396−7405.
(64) Scurlock, C. T.; Pullins, S. H.; Duncan, M. A. Photodissociation Spectroscopy of Ca^+CO_2. *J. Chem. Phys.* **1996**, *105*, 3579−3585.
(65) Iskra, A.; Gentleman, A. S.; Kartouzian, A.; Kent, M. J.; Sharp, A. P.; Mackenzie, S. R. Infrared Spectroscopy of Gas-Phase $M^+(CO_2)_n$ (M = Co, Rh, Ir) Ion−Molecule Complexes. *J. Phys. Chem. A* **2017**, *121*, 133−140.

DOI: 10.1021/acs.jpca.8b01843
J. Phys. Chem. A 2018, 122, 2983−2991